Quasiatomic Fine Structure and Selection Rules in Quantum Dots

C. Schüller, K. Keller, G. Biese, E. Ulrichs, L. Rolf, C. Steinebach, and D. Heitmann
Institut für Angewandte Physik und Zentrum für Mikrostrukturforschung, Universität Hamburg, Jungiusstraße 11, D-20355 Hamburg, Germany

K. Eberl
Max-Planck-Institut für Festkörperforschung, Heisenbergstraße 1, D-70569 Stuttgart, Germany
(Received 8 August 1997)

We probe the electronic shell structure of quasiatomic systems, realized in GaAs-AlGaAs quantum dots, by resonant Raman spectroscopy. We observe a series of discrete spin-density excitations, whose energies are very close to single-particle level spacings in a quantum dot. The combined information from experiments at different wave vectors in the lateral direction and from investigations with applied magnetic fields reveals a distinct set of Raman allowed transitions $(\Delta n, \Delta m)$, where changes Δn and Δm are changes in radial and angular momentum quantum numbers, respectively. [S0031-9007(98)05571-9]

PACS numbers: 73.20.Dx, 71.45.Gm, 73.20.Mf, 78.55.Cr

Modern sophisticated growth techniques for semiconductor structures, such as molecular-beam epitaxy in combination with the technique of modulation doping have made it possible to realize nearly perfect two-dimensional (2D) electron gases in semiconductor heterostructures or quantum wells. Such structures are ideal starting points to fabricate systems with further reduced dimensionality, e.g., quantum wires and quasi-zero-dimensional (0D) dots. The latter can be considered as some kind of artificial atoms. The electronic excitations in these 0D systems can be probed advantageously by resonant Raman spectroscopy. In zinc blende-type semiconductors one can excite collective charge-density excitations (CDE, plasmons), which energies are renormalized with respect to single-particle energy spacings due to direct and exchange Coulomb interactions. One can also excite collective spin-density excitations (SDE) [1], which are affected only by exchange interaction and are therefore redshifted with respect to the corresponding single-particle energies [2,3]. The CDE and SDE can be distinguished by polarization selection rules. CDE are observed if the polarizations of the incoming and scattered light are parallel to each other (polarized geometry) and SDE if the polarizations are perpendicular (depolarized geometry). There is a number of interesting Raman investigations of modulation-doped quantum-dot structures with [4] and without [3,5] external magnetic field. Lockwood *et al.* [4] recently found evidence for the shell structure in quantum dots by comparing single-particle excitations (SPE), so called since they occur in both polarization geometries [2], with a self-consistent Hartree calculation. We present in this Letter measurements on high-quality GaAs-AlGaAs quantum dots where we preserve polarization selection rules and can resolve in one and the same quantum-dot sample in addition to the SPE the spectrum of collective CDE and SDE in dependence on the transferred lateral wave vector q and magnetic field B. In contrast to the SPE, these excitations are very sharp and allow a fundamental investigation. At $B = 0$, we find for large q a detailed fine structure in the spectrum of the SDE's. At $B > 0$, we observe a characteristic splitting of the lowest SDE mode, the SDE_1. The low-frequency branch has a negative B dispersion and represents a collective edge-spin-density mode. The SDE_1 has a much lower energy than the CDE_1 mode, the Kohn's mode [6], and its energy is very close to the single-particle level spacing between the highest occupied and the first unoccupied level in the quantum dot. Interestingly, the second spin-density mode, the SDE_2, shows no significant energy shift with B. The analysis of this behavior, in combination with our investigations at various wave vectors q, allows us to identify the involved single-particle transitions. They take place between different electronic shells and resemble an atomic fine structure. Our investigations give a complementary view of the recent investigations of quantum dot atoms by transport and capacitance spectroscopy (e.g., Refs. [7–9]).

For our studies we have prepared arrays of deep-etched quantum dots by holographic lithography and reactive-ion etching on one-sided modulation-doped GaAs-$Al_{0.3}Ga_{0.1}As$ single quantum wells with 25 nm well width. The carrier densities and mobility of the quantum well samples were in the range of $(7-8) \times 10^{11}$ cm^{-2} and 7×10^5 cm^2 V^{-1} s^{-1}, respectively. The lateral dot diameters were in the range of 170–250 nm. Raman experiments have been performed in a closed-cycle cryostat at $T = 12$ K, and at $T = 2$ K in a split-coil magnet.

Raman spectra of a quantum dot sample with 240 nm dots are shown in Fig. 1. To transfer a wave vector q in the lateral direction, the sample normal was tilted with respect to the directions of incoming and scattered light. Three well pronounced peaks can be observed in the depolarized geometry at large q [Fig. 1(a)]. From the polarization selection rules these peaks can be identified

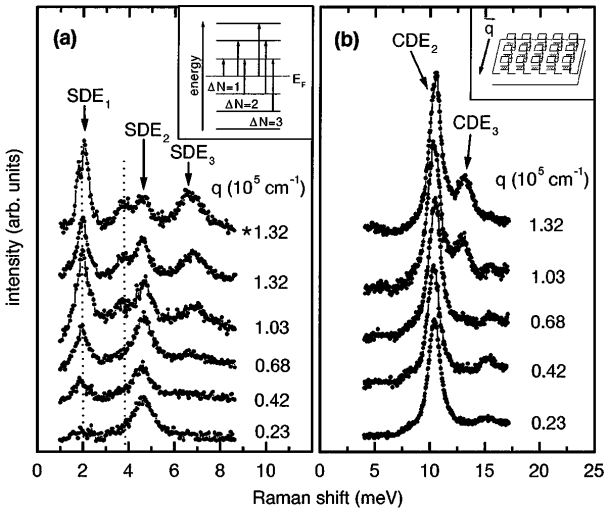

FIG. 1. (a) Depolarized and (b) polarized Raman spectra of a quantum dot sample with 240 nm dot diameter for different wave-vector transfer q. The depolarized spectra in (a) were recorded at a laser energy $E_L = 1600.7$ meV, the spectrum marked with (*) at $E_L = 1601.3$ meV. The insets sketch (a) those single-particle transitions which predominantly contribute to the observed excitations, and (b) the direction of wave-vector transfer.

as SDE's. As we will see below, the energies of these collective SDE's are very close to single-particle level spacings in the dots, as sketched in the inset in Fig. 1(a). Energy renormalizations due to collective effects are about 10%. Thus it may be justified to compare these excitations in the depolarized spectra with the single-particle spectrum of a quantum dot, neglecting the small collective effects for a moment. In accordance with Ref. [5], we can attribute the first peak (SDE_1) to single-particle transitions from the highest occupied to the first unoccupied level in the quantum dot, the second peak (SDE_2) to transitions with $\Delta N = 2$, and for the third peak $\Delta N = 3$, as sketched in the inset.

The polarized spectra in Fig. 1(b) exhibit a very strong CDE_2 peak and, for $q \geq 1 \times 10^5$ cm^{-1}, a weaker CDE_3. The large difference in energetic positions between the CDE_i and SDE_i is due to many-particle interactions [3]. At small q we observe only one peak, both for the depolarized and the polarized spectra. Considering general aspects of Raman scattering one can say that in a symmetric system the Raman allowed excitations have even parity because the Raman process is a two-photon process. This implies that the excitation at 4.5 meV in the depolarized spectra (labeled SDE_2) and the one at 10.5 meV in the polarized spectra (labeled CDE_2) have even parity. The symmetries of the excitations are broken by applying a wave-vector transfer in the lateral direction and Raman forbidden excitations with odd parity occur. From the depolarized spectra at large wave vector $q = 1.32 \times 10^5$ cm^{-1} three remarkable facts can be extracted. (i) At the low-energy side of the SDE_2 an additional peak occurs. By slightly changing the laser energy and thereby the resonant conditions (spectrum with an asterisk), this additional peak can be resonantly enhanced. (ii) The SDE_1, SDE_2, and the additional peak have essentially the same linewidth ($\approx$0.5 meV), whereas the SDE_3 has more than twice the linewidth of the other peaks ($\approx$1.1 meV), and (iii) the energetic position of the additional peak is almost exactly twice that of the SDE_1 (marked with vertical dashed lines). We will come back to this interesting point below when we discuss the results of the experiments in a magnetic field.

The spectra discussed so far were taken from extensive series of measurements for many different laser frequencies well above the band gap, where the spectra are dominated by the collective excitations. We note that, if we tune the laser frequency close to the effective band gap of the system, i.e., under conditions of extreme resonance, the spectra are dominated by SPE's, which occur in both polarizations and are very similar to the excitations observed in Ref. [4]. For illustration, we compare in the left panel of Fig. 2 these SPE-dominated spectra with SDE- and CDE-dominated spectra. In the right panel we discuss the experimental dispersions of SDE's (solid symbols) and CDE's (open symbols) in an external magnetic field. We find that in a magnetic field plasmons can also be observed in the depolarized geometry. The open triangles in Fig. 2 correspond to CDE's which are most pronounced in depolarized spectra and the open squares to CDE's which are dominant in polarized scattering geometry. Our SPE's have a half-width of 1.5 meV, about half the linewidth reported in Ref. [4]. We find that the SDE's are even sharper ($\approx$0.5 meV), which allows us to do a detailed study of the dynamic

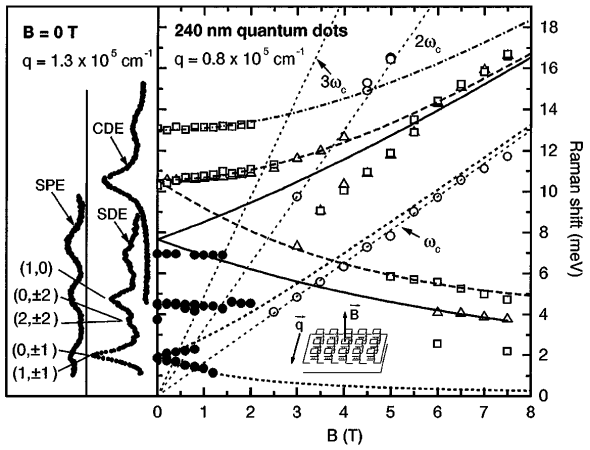

FIG. 2. B dispersions of SDE's (solid symbols) and CDE's (open symbols) in a quantum-dot sample. In the left panel spectra of SDE's and CDE's for $B = 0$ are displayed, which were taken at $E_L = 1587$ meV. The spectrum of SPE's was recorded at a laser energy $E_L = 1561$ meV under conditions of extreme resonance. For better comparison we have subtracted from this spectrum the hot luminescence background.

excitations in the quantum systems. We note here that for measurements at $B > 0$ in the split-coil magnet we have to use glancing incidence of the laser beam onto the sample from a side window to realize a finite wave-vector transfer in the lateral direction if the magnetic field is oriented parallel to the sample normal. Therefore we are restricted to a value of $q = 0.8 \times 10^5$ cm^{-1} for the wave-vector transfer. Thus we cannot follow all excitations, in particular, also the SPE's, at $B = 0$ to higher B.

We do not want to elaborate in detail on the observed magnetoplasmon modes (open symbols in Fig. 2) because this point is well known from far infrared (FIR) experiments [6,10,11]. We rather want to concentrate on the SDE's (solid symbols) in Fig. 2. The SDE_1 splits into two branches at finite magnetic field. Interestingly the SDE_2 shows neither a significant splitting nor an energy shift with magnetic field. The signals corresponding to the SDE_3 are very weak and broad so that we cannot definitely say if there is a splitting or not. We find for all observed spin-density excitations that their intensities drop drastically with increasing magnetic field and at fields above 2 T they can no longer be resolved.

In the following we want to discuss and interpret our observations in a simple qualitative model. It is well known from FIR experiments and theoretical considerations on modulation-doped deep-etched structures that the external lateral potential is to a good approximation parabolic [10]. Therefore we can in a first approach assume that also the effective (screened) potential of our quantum dot is parabolic. The energies for an electron in a two-dimensional parabolic potential with external magnetic field are given by

$$E_{n,m} = (2n + |m| + 1)\hbar\sqrt{\Omega_0^2 + \left(\frac{\omega_c}{2}\right)^2} + m\hbar\,\frac{\omega_c}{2}\,. \tag{1}$$

Here n is the so called radial and m the azimuthal or angular momentum quantum number; Ω_0 is the quantization energy. In Fig. 3(a) the spectrum (solid squares) corresponding to Eq. (1) is displayed for $B = 0$, i.e., $\omega_c = 0$. The lines connect points which belong to the same n. The radial quantum number $n = 0, 1, 2, \ldots$ rises from the bottom to the top. With, e.g., the labels "s" or "p," we have indicated the character of the quasiatomic shells as quasi-s or quasi-p orbitals, respectively. We call it *quasi* because the symmetries of these quantum dot orbitals are different from that of real 3D atoms. From geometrical considerations we can estimate the number of electrons per dot in our structure to be about 200. For simplicity, in Fig. 3 we have considered 42 electrons per dot but this makes no qualitative difference in our interpretation. Considering Eq. (1), one can easily see that here the lateral quantum number N, in the inset in Fig. 1, is defined by $N = 2n + |m| + 1$. In the case $\Delta N = 1$ we can make transitions from the highest occupied level [horizontal dashed line in Fig. 3(a)] to the next higher level. This means, e.g., transitions with $(\Delta n = 0, \Delta m = \pm 1)$ or $(\Delta n = 1\Delta, m = \pm 1)$ as marked by the solid arrows in Fig. 3(a). Correspondingly, this also implies that the transitions take place between orbitals with different symmetry or parity. Figure 3(b) displays the corresponding result for a finite magnetic field $B = 0.5$ T. As indicated by the solid arrows we can see that some transition energies decrease while others increase with increasing B. Concerning our experimental observation this gives the correct result: The two dotted lines, starting at 2 meV at $B = 0$ in Fig. 2, mark the transition energies calculated with Eq. (1) for $(\Delta n = 0, \Delta m = \pm 1)$ and $(\Delta n = 1, \Delta m = \pm 1)$ which are energetically degenerate [see also Fig. 3(d)]. In this parabolic model the splitting between the two branches is exactly ω_c. We note here that this situation is the analog to the splitting of the Kohn's mode in a magnetic field. The crucial difference is that the Kohn's mode represents the quantization energy of the external potential, whereas here the SDE_1 represents approximately the single-particle energy spacing of the screened lateral potential. This analogy leads us to the interpretation that the excitation of the lower branch is an edge spin-density mode where the electrons perform skipping-orbit motions at the edge of the dot. The slight deviation of the experimental points in the upper branch from

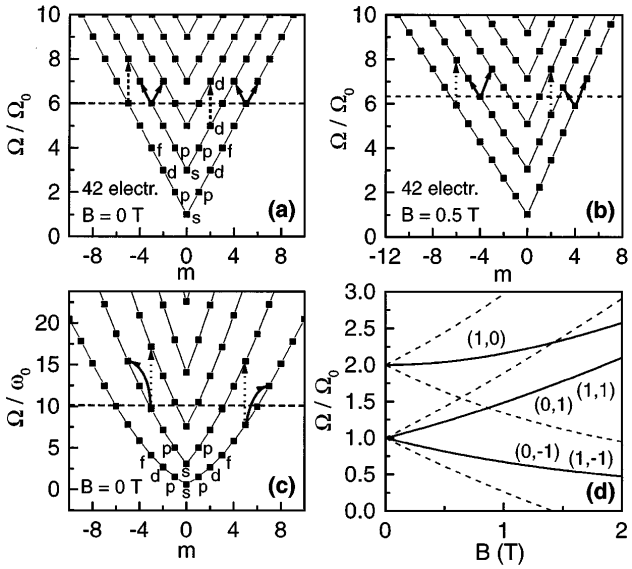

FIG. 3. Calculated energies for a quantum dot with parabolic effective potential without (a) and with (b) external magnetic field. (c) Calculated energies in a dot with cylindrical symmetry and hard walls. (d) Single-particle transition energies for a parabolic quantum dot with external magnetic field. The solid lines mark the experimentally observed transitions; the dashed lines give the forbidden next higher transitions. For the two dashed lines starting at $\Omega/\Omega_0 = 1$ the corresponding transitions are $(-1, \pm 3)$ and $(2, \pm 3)$, for the dashed lines starting at $\Omega/\Omega_0 = 2$, $(0, \pm 2)$, and $(2, \pm 2)$. In a hard-wall potential, the $(0, \pm 2)$ and $(2, \pm 2)$ are shifted to lower energies and are causing a fine structure. Ω_0 characterizes the parabolic potential, $\omega_0 = (\hbar/2m^*)(\pi/a)^2$, with a being the dot diameter, characterizes the hard-wall potential.

the calculated line can be attributed to a nonparabolicity in the real effective potential or to an effect of the so far neglected collective nature of the excitations. The collective nature of the SDE's can furthermore be deduced from the observed vanishing of the excitations at relatively small magnetic fields. This can be understood as an effect of Landau damping: At finite magnetic field all degeneracies are lifted and several single-particle transitions with different energies are possible. The single-particle lines cross the energies of the SDE so that they get Landau damped. For illustration, the forbidden next higher transitions are displayed in Fig. 3(d) (dashed lines).

For the SDE_2, in principle, also several transitions are possible which can easily be seen in Fig. 3(a). But from our experimental observations we deduce that only one type of excitation may significantly contribute to the experimentally observed SDE_2 peak: transitions with $(\Delta n = 1, \Delta m = 0)$. In other words, transitions between orbitals with the same symmetry, e.g., from quasi-s to quasi-s orbitals or from quasi-p to quasi-p orbitals, and so on, which is again characteristic of the two-photon Raman process. Some transitions are marked by dashed arrows in Fig. 3(a). All other possible transitions have $|\Delta m| \geq 2$. In a magnetic field, this results in splittings $\geq 2\omega_c$ [see dashed lines in Fig. 3(d)] which are experimentally not observed. Only the $(\Delta n = 1, \Delta m = 0)$ transition has a moderate increase with magnetic field and no splitting as displayed in Fig. 3(d). The fact that we do not observe an increase in energy may be explained, as in the case of the SDE_1, to arise either from nonparabolicity or from the collective nature of the SDE_2.

At large q, we observe at $B = 0$ an additional fine structure at 4 meV [Fig. 1(a)]. We cannot follow this peak in the magnetic field experiments because of the limited accessible q vectors in the split-coil magnet. At $B > 0$, we could resolve only the strong SDE_2 peak. We now claim that the additional peak just stems from the transitions with $\Delta m = \pm 2$. In the parabolic model the transitions with $(\Delta n = 0, \Delta m = \pm 2)$ (additional peak) and $(\Delta n = 1, \Delta m = 0)$ (SDE_2) are energetically degenerate at $B = 0$. The real dot potential would certainly deviate from a parabolic shape because we have approximately 200 electrons in the dot and screening should be important. So the other extreme limit would be a hard-wall potential. The real potential should be somewhere in between these two limits. In Fig. 3(c) we have calculated the energy spectrum for a hard-wall potential with cylindrical symmetry. From this diagram we can extract two essential results: (i) Transitions with $(\Delta n = 0, \Delta m = \pm 2)$ (solid arrows) have lower energies than transitions with $(\Delta n = 1, \Delta m = 0)$ (dotted arrows). This explains the energetic position of the additional peak in Fig. 1. (ii) Transitions with $(\Delta n = 0, \Delta m = \pm 2)$ (additional peak) have a very good approximation twice the energy of transitions with $(\Delta n = 0, \Delta m = \pm 1)$ (SDE_1) even in the case of the hard-wall potential. This is indeed observed in the experiments and marked by the two vertical lines in Fig. 1. For clarity, we have labeled the peaks in the experimental spectra in the left panel of Fig. 2 with the corresponding transitions.

In conclusion, from our investigations it follows that in quantum dots dominantly transitions with changes in quantum numbers $\Delta n, |\Delta m| \leq 1$ contribute to the collective low-energy SDE's, whereas transitions with $\Delta n, |\Delta m| \leq 2$ are observed only at relatively large wave-vector transfer q and form a fine structure. We have observed all types of elementary electronic excitations in one and the same quantum dot sample. This opens the possibility for detailed theoretical studies of the dynamic response, including the very interesting exchange-correlation effects.

We thank Vidar Gudmundsson for valuable discussions. This work was supported by the Deutsche Forschungsgemeinschaft via the Graduiertenkolleg "Physik nanostrukturierter Festkörper" and Projects No. He1938/6 and He1938/7.

[1] For an overview, see A. Pinczuk and G. Abstreiter, in *Light Scattering in Solids V*, Topics in Applied Physics Vol. 66, edited by M. Cardona and G. Güntherodt (Springer, Berlin, 1988), p. 153.
[2] A. Pinczuk, S. Schmitt-Rink, G. Danan, J. P. Valladares, L. N. Pfeiffer, and K. W. West, Phys. Rev. Lett. **63**, 1633 (1989).
[3] C. Schüller, G. Biese, K. Keller, C. Steinebach, D. Heitmann, P. Grambow, and K. Eberl, Phys. Rev. B **54**, R17 304 (1996).
[4] D. J. Lockwood, P. Hawrylak, P. D. Wang, C. M. Sotomayor Torres, A. Pinczuk, and B. S. Dennis, Phys. Rev. Lett. **77**, 354 (1996).
[5] R. Strenz, U. Bockelmann, F. Hirler, G. Abstreiter, G. Böhm, and G. Weimann, Phys. Rev. Lett. **73**, 3022 (1994).
[6] T. Demel, D. Heitmann, P. Grambow, and K. Ploog, Phys. Rev. Lett. **64**, 788 (1990).
[7] R. C. Ashoori, H. L. Stormer, J. S. Weiner, L. N. Pfeiffer, K. W. Baldwin, and K. W. West, Phys. Rev. Lett. **71**, 613 (1993).
[8] R. C. Ashoori, Nature (London) **379**, 413 (1996).
[9] S. Tarucha, D. G. Austing, T. Honda, R. J. van der Hage, and L. P. Kouwenhoven, Phys. Rev. Lett. **77**, 3613 (1996).
[10] D. Heitmann and J. P. Kotthaus, Phys. Today **46**, No. 6, 56 (1993), and references therein.
[11] V. Gudmundsson, A. Brataas, P. Grambow, B. Meurer, T. Kurth, and D. Heitmann, Phys. Rev. B **51**, 17 744 (1995).